Construction and Building Materials 264 (2020) 120708

Contents lists available at ScienceDirect

Construction and Building Materials

journal homepage: www.elsevier.com/locate/conbuildmat

Modelling of autogenous shrinkage of hardening cement paste

Tianshi Lu *, Zhenming Li, Klaas van Breugel

Department of Materials, Mechanics, Management & Design, Faculty of Civil Engineering and Geoscience, Delft University of Technology, Delft, the Netherlands

HIGHLIGHTS

- A simulation model for autogenous deformation is proposed.
- Investigation of the role of creep on autogenous shrinkage.
- Experimental investigation of early age properties of cement pastes.
- Experimental and numerical study of the autogenous shrinkages of Portland cement paste and BFS cement paste.

ARTICLE INFO

Article history:
Received 22 June 2020
Received in revised form 17 August 2020
Accepted 21 August 2020

Keywords:
Autogenous shrinkage
Cement
Blast furnace slag
Creep
Activation energy
Modelling

ABSTRACT

In recent decades, several simulation models have been proposed to predict autogenous shrinkage of cementitious systems. In most of these models, however, only the elastic deformation caused by self-desiccation of the hydrating cement paste is considered. In fact, cement paste is not an ideal elastic material. Also the time-dependent deformation, i.e. creep, has been proposed an important component of autogenous shrinkage, especially at the early age. In this study, a simulation model for autogenous deformation is proposed, which includes an elastic part and a time-dependent part. The time-dependent part of this model is based on the activation energy concept. The capillary tension is considered as the driving force of the autogenous shrinkages. In order to evaluate the accuracy of the prediction with the proposed model, CEM I and CEM III/B pastes are studied in this paper. The simulated autogenous shrinkages are compared with experimental results.

1. Introduction

Durability of infrastructures has become a more and more important issue. Many structures are in serious need of repair, retrofitting or replacement, after a certain service period. There are many factors affecting the long-term performance of cementitious materials. Early-age cracking is one of these factors designers have to deal with. Cracks may promote degradation of the concrete due to chemical and microbiological processes, e.g. sulphate attack, corrosion of reinforcing steel and alkali-silica reaction. Restrained shrinkage is one of the major causes of early-age cracking in concrete structures. Restraint can be external, e.g. caused by adjoining structures, or internal, caused by the reinforcement [1], non-shrinking aggregates [2] of non-linear strain gradients.

There are many different types of shrinkage of concrete, e.g. temperature induced shrinkage, drying shrinkage and autogenous shrinkage. Among these types of shrinkage, autogenous shrinkage is a consequence of self-desiccation during the cement hydration process. For a long time autogenous shrinkage was considered negligible compared with drying shrinkage. In recent years, autogenous shrinkage has drawn more and more attention due to the increasing use of high-performance concrete, which is generally produced with a low water-cement ratio and contains supplementary cementitious materials. In the meantime, many researches of autogenous shrinkage have been done [3,4], but the mechanism behind autogenous shrinkage is not fully understood yet [5]. There is a general agreement about the existence of a relationship between autogenous deformation and relative humidity change in the capillary pores of the hardening cement paste. A few simulation models were built based on this theory [5–9]. In those simulation models, cementitious systems were considered elastic materials, and autogenous shrinkage was modelled as a function of the internal relative humidity. However, simulations often show discrepancies between the measured and calculated autogenous deformations. At later ages these discrepancies become more pronounced [8]. A few researchers believed that these discrepancies are caused by the time-dependent behavior of the material, i.e. creep [8,10–14]. Many mechanisms of creep and creep-promoting factors have been proposed in past decades [15,16],

* Corresponding author.
E-mail address: Lutianshi2017@gmail.com (T. Lu).

https://doi.org/10.1016/j.conbuildmat.2020.120708
0950-0618/

e.g. viscous flow and micro-cracking. Although no single theory proposed so far describes the creep phenomena comprehensively, the mechanisms proposed in the past have one thing in common: they are all related predominantly to the microstructure and water content of the cement paste and to changes thereof [17].

In order to simulate the creep part of autogenous shrinkage, different formulae and simulation models have been developed in the past few years [18,19]. But most of these models are empirical and based on experimental data. They can only be used to simulate the creep part of autogenous shrinkage of a limited number of mixtures and for a limited period of time. In this paper, a theoretical simulation model for autogenous deformation is proposed that includes an elastic part and a time-dependent part. The time-dependent part of this model is based on the activation energy concept and extended to deal with the continuously changing physical properties of hardening cement paste. The proposed model is applied for predicting autogenous deformation of a Portland cement paste (CEM I 42.5 N) and a blast furnace slag cement paste (CEM III 42.5 N). The simulated autogenous shrinkages are compared with the experimental results.

2. Theoretical basis of this study

2.1. Deformation of hardening cement paste under load

The deformation of cement paste under load can be divided into two parts, an elastic part and a time-dependent part, as shown in Fig. 1. In formula form:

$$\varepsilon(t,\ \tau)\ =\ \varepsilon_{el}\ (\tau)\ +\varepsilon_{cr}(t,\ \tau) \tag{1}$$

where $\varepsilon(t,\tau)$ [m/m] is the total deformation at time t; $\varepsilon_{el}(\tau)$ [m/m] the elastic deformation at loading time τ; $\varepsilon_{cr}(t,\tau)$ [m/m] the time-dependent deformation at time t, which is called creep;τ the time at loading.

2.1.1. Elastic deformation $\boldsymbol{\varepsilon_{el}(\tau)}$

The elastic deformation $\varepsilon_{el}(\tau)$ can be calculated as [20]:

$$\varepsilon_{el}(\tau)=\frac{\sigma(\tau)}{E(\tau)}(1-2\vartheta)=\frac{\sigma(\tau)}{3K_P(\tau)} \tag{2}$$

where $\sigma(\tau)$[MPa] is the applied stress at time τ;$E(\tau)$ [MPa] elastic modulus of cement paste at time τ; ϑ is the Poisson's ratio, for cement paste its value is taken as 0.2 [21]; $K_P(\tau)$ is the bulk modulus of the cement paste at time τ. $K_P(\tau)$ can be calculated using the following formula [22]:

$$K_P(\tau)=\frac{E(\tau)}{3(1-2\vartheta)} \tag{3}$$

2.1.2. Time-dependent deformation $\boldsymbol{\varepsilon_{cr}(t,\tau)}$

In this paper, the activation energy concept will be applied to calculate the time-dependent part of autogenous deformation. Many researchers have used the activation energy concept to calculate the creep of cementitious materials [23–26]. For a hardened cement paste under constant load, the time-dependent strain of the cement paste specimen can be written as [27,28]:

$$\varepsilon_{cr}(t,\tau)=\frac{2\sigma(\tau)}{E(\tau)}\left(1-\exp\left(-\frac{\omega\eta E(\tau)}{2\exp\left(\frac{Q(t)}{RT}\right)}t\right)\right) \tag{4}$$

where $Q(t)$ [KJ/mol] is the activation energy of the cement paste; ω [-] and η [m²/N] are structure dependent parameters and are constant for a given material. Their values are taken as 0.03 and 4.8 × 10^{-8} m²/N, respectively[29]; $\sigma(\tau)$ is the stress at time τ; $E(\tau)$ [MPa] the elastic modulus of cement paste at time τ; τ the time at loading; R [J/(mol · K)] the universal gas constant and T [K] the absolute temperature.

Based on Equation (4), the rate of creep can be written as [27]:

$$\dot{\varepsilon}_{cr}(t,\tau)=\omega\eta\sigma(\tau)exp\left(-\frac{Q(t)}{RT}\right) \tag{5}$$

For early-age autogenous shrinkage of cement paste, the internal load related to self-desiccation during the cement hydration process, e.g. capillary tension, increases with the drop of relative humidity. In the meantime, the elastic modulus increases. For simulating the time-dependent part of early-age autogenous shrinkage, the changing physical properties of cement paste, which are related to the changing microstructure, should be taken into consideration. As schematically shown in Fig. 2, the time-dependent part of autogenous shrinkage $\varepsilon_{cr}(t_n,\tau_n)$ is the summation of increments of creep that were formed at subsequent time intervals, e.g. from τ_{n-1} to τ_n. It can be expressed as:

$$\varepsilon_{cr}(t_n,\tau_n)=\sum_{k=1}^{n-1}\Delta\varepsilon_{cr}(t_k,\tau_k) \tag{6}$$

where $\Delta\varepsilon_{cr(t_k,\tau_k)}$ is the increment of creep from τ_k to τ_{k+1}. With the increase of index k, time τ_k increases as shown in Fig. 2, e.g. τ_{n-1} and τ_n.

At time τ_n, the internal stress causing autogenous shrinkage is $\sigma(\tau_n)$. As shown in Fig. 2, the increasing rate of creep $\dot{\varepsilon}_{cr}(t_n,\tau_n)$ at τ_n can be calculated with Equation (5) [25]:

$$\dot{\varepsilon}_{cr}(t_n,\tau_n)=\omega\eta\sigma(\tau_n)exp\left(-\frac{Q(t_n)}{RT}\right) \tag{7}$$

According to Wittmann [29], the activation energy $Q(t_n)$ can be expressed as:

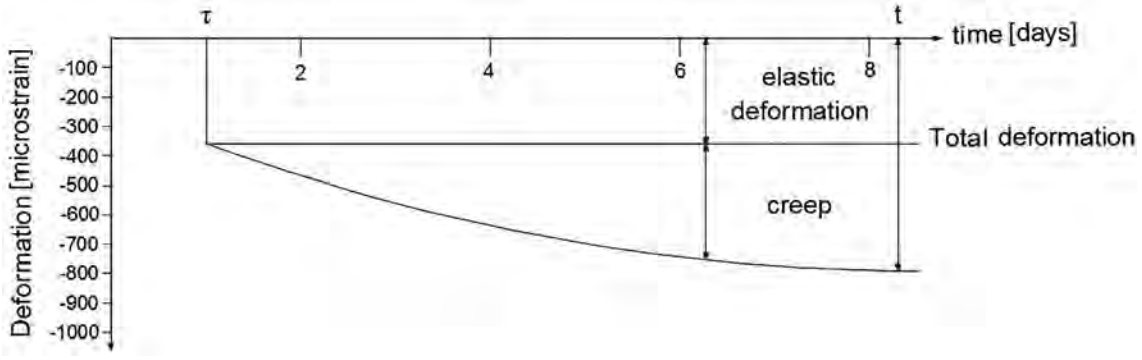

Fig. 1. Schematic representation of deformation of the cement paste under load.

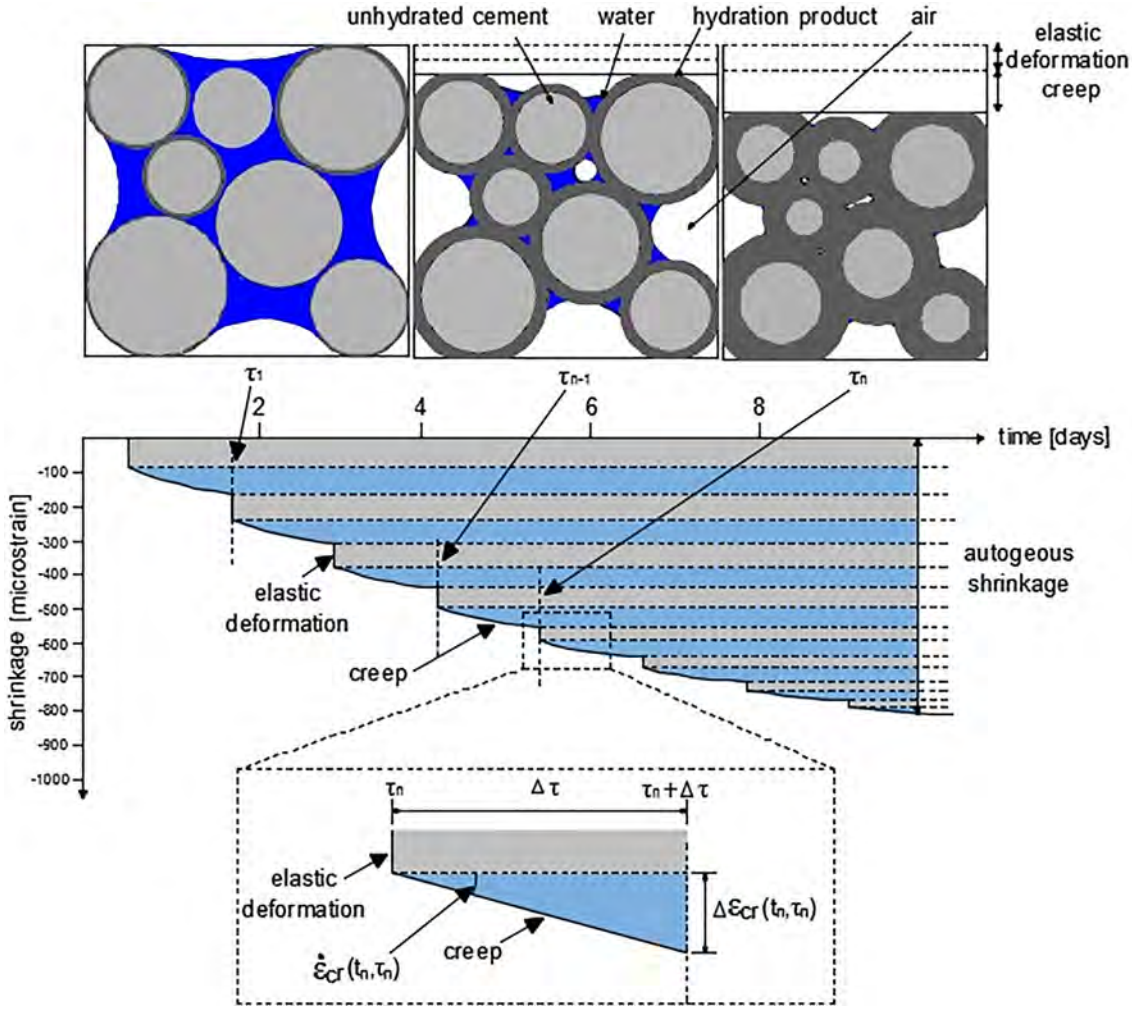

Fig. 2. Schematic representation of autogenous shrinkage of hardening cement paste.

$$Q(t_n) = Q_0 + mlnt_n \tag{8}$$

where $mlnt_n$describes the evolution of the activation energy with time. In this paper, the value of activation energy Q_0 is taken as 15 KJ/mol and m is taken as 1.4 KJ/mol [29,30].

The increment of creep $\Delta\varepsilon_{cr}(t_n, \tau_n)$ (as shown in Fig. 2) from time τ_n to time $\tau_n + \Delta\tau$ can be calculated as:

$$\Delta\varepsilon_{cr}(t_n, \tau_n) = \dot{\varepsilon}_{cr}(t_n, \tau_n)\Delta\tau = \omega\eta\sigma(\tau_n)\exp\left(-\frac{Q(t_n)}{RT}\right)\Delta\tau \tag{9}$$

The creep $\varepsilon_{cr}(t_{n+1}, \tau_{n+1})$ at time $\tau_n + \Delta\tau$ can be calculated as the summation of increments of creep:

$$\begin{aligned}\varepsilon_{cr}(t_{n+1}, \tau_{n+1}) &= \varepsilon_{cr}(t_n, \tau_n) + \Delta\varepsilon_{cr}(t_n, \tau_n) \\ &= \sum_{k=1}^{n-1}\Delta\varepsilon_{cr}(t_k, \tau_k) + \omega\eta\sigma(\tau_n)exp\left(-\frac{Q(t_n)}{RT}\right)\Delta\tau\end{aligned} \tag{10}$$

2.2. Internal load of autogenous shrinkage

2.2.1. Mechanism for autogenous shrinkage

Many studies have been carried out on the mechanism of autogenous shrinkage. So far no consensus has been reached about the cause of autogenous shrinkage. Disjoining pressure, change in the surface tension of the solid gel particles and capillary tension are considered as the three principal mechanisms. According to Wittmann [31] and Setzer [32], surface tension of the solid does not contribute much to the autogenous shrinkage when the relative humidity is higher than 50%. In early-age cement paste, the relative humidity due to self-desiccation alone does not drop below 75% [33]. Therefore, surface tension in solid particles is not the mechanism of autogenous shrinkage. Some researchers consider disjoining pressure as the dominant mechanism of autogenous shrinkage [34], while others think that capillary tension is the dominant mechanism [10,35]. The disjoining pressure is repulsion-dominated and its magnitude increases with decreasing pore size. The disjoining pressure separates the adjacent cement particles in cement paste and it has a significant magnitude in small gel pores where reaction products are densely packed [14]. Meanwhile, the pore water in capillary pores is in tension and puts the solid skeleton of cement paste, including the water between reaction products, in compression, which results in an external volume reduction of the cement paste, i.e. autogenous shrinkage. Capillary tension increases with decreasing internal relative humidity. In cement paste the compressive forces must be in equilibrium with tensile forces. It is assumed, therefore, that capillary tension and disjoining pressure are related. If this assumption holds, either disjoining pressure or capillary tension can be adopted as parameter for describing autogenous shrinkage [36]. In this paper, the calculated capillary tension is used to predict the autogenous shrinkage of cement paste.

With the drop of internal relative humidity, caused by self-desiccation of hydrating cement paste, the capillary tension

increases. The radius of the largest capillary pore filled with water at certain internal relative humidity can be calculated as [37,38]:

$$r = -\frac{2\gamma V_w}{RT\ln\frac{RH}{RH_S}} \tag{11}$$

where γ [N/m] is the surface tension of the pore fluid, 0.073 N/m for pure water; V_w [m³/mol] the molar volume of water, 18.02×10^{-6}m³/mol; R[J/(molÂ · K)] the ideal gas constant, 8.314J/(molÂ · K); T[K] the absolute temperature; RH the measured relative humidity and RH_S the effect of dissolved ions on relative humidity, in this paper, its value is taken as 0.97 [14].

According to the Laplace law [39], the capillary tension σ_{cap} [MPa] in the pore fluid can be calculated as (in this paper, tension is defined as negative and compression is defined as positive):

$$F_c = -\frac{2\gamma}{r}\sigma_{cap} = -\frac{2\gamma}{r} \tag{12}$$

2.2.2. Effective stress

The internal pressure exerted by the pore water on the solid phase is called effective stress (called also Skempton's stress [40]). According to Gray et al. [41], the effective stress σ_e [MPa] can be written as:

$$\sigma_e = \kappa p^s I \tag{13}$$

where I [–] is the unit tensor of second order; p^s [MPa] is the internal pressure exerted by the pore water on the solid phase; κ [-] is the Biot coefficient. The Biot coefficient describes to which extent the internal pressure causes the deformation of porous materials [42]. It can be written as:

$$\kappa = 1 - K_P/K_S \tag{14}$$

where K_S [MPa] is the bulk modulus of the solid skeleton of cement paste, its value is taken as 44 GPa [21]; K_P [MPa] the bulk modulus of the cement paste.

For early-age autogenous shrinkage of cement paste, only the internal pressure exerted by the pore water, p^s, acts on the solid phase (Fig. 3). Due to the exerted internal pressure, the solid skeleton of the cement paste is under compression and the volume of cement paste decreases.

As mentioned earlier in this paper, capillary tension is considered as the major internal driving force of autogenous shrinkage. According to Gawin et al. [12], in this case, the internal pressure p^s can be written as:

$$p^s = S_w\sigma_{cap} \tag{15}$$

where σ_{cap} [MPa] the capillary tension and S_w [–] is the degree of saturation, which can be calculated as the ratio between the evaporable water content in the hardening paste, V_{ew} [cm³ water / cm³ paste], and the total pore volume of the paste (capillary pore and gel pore), V_p [cm³ pore / cm³ paste] [43]:

$$S_w = \frac{V_{ew}}{V_p} = \frac{V_{iw} - V_{new}}{V_{iw} - V_{new} + V_{cs}} \tag{16}$$

where V_{iw} [cm³ water / cm³ paste] is the initial water content; V_{new} [cm³ non-evaporable water / cm³ paste] the non-evaporable water content and V_{cs}[cm³ chemical shrinkage / cm³ paste] the volume of chemical shrinkage.

The effective stress σ_e in one direction can be written as [7,12]:

$$\sigma_e = \kappa S_w\sigma_{cap} \tag{17}$$

Note that the capillary tension σ_{cap} is multiplied by the degree of saturation S_w to calculate the effective stress in Equation (17). All the pores filled with water in cement paste are considered as capillary pore. In reality, part of the pores filled with water in cement paste is gel pore [44]. According to Zeng et al. [45] who measured the pore size distribution of Portland cement paste with water-binder ratio of 0.3, the proportion of gel pore at seven days is about 10% of the total pore volume [45]. Therefore, the effective stress σ_e calculated by Equation (17) is a virtual stress [7] and discrepancy is about 10%.

2.3. Calculation of autogenous shrinkage of cement paste

The autogenous shrinkage of hardening cement paste can be calculated as the sum of the elastic and the creep part:

$$\varepsilon(t,\tau) = \varepsilon_{el}(\tau) + \varepsilon_{cr}(t,\tau) = \frac{S_w(\tau)\sigma_{cap}(\tau)}{3}\left(\frac{1-2\vartheta}{E(\tau)} - \frac{1}{K_S}\right) + \tag{18}$$

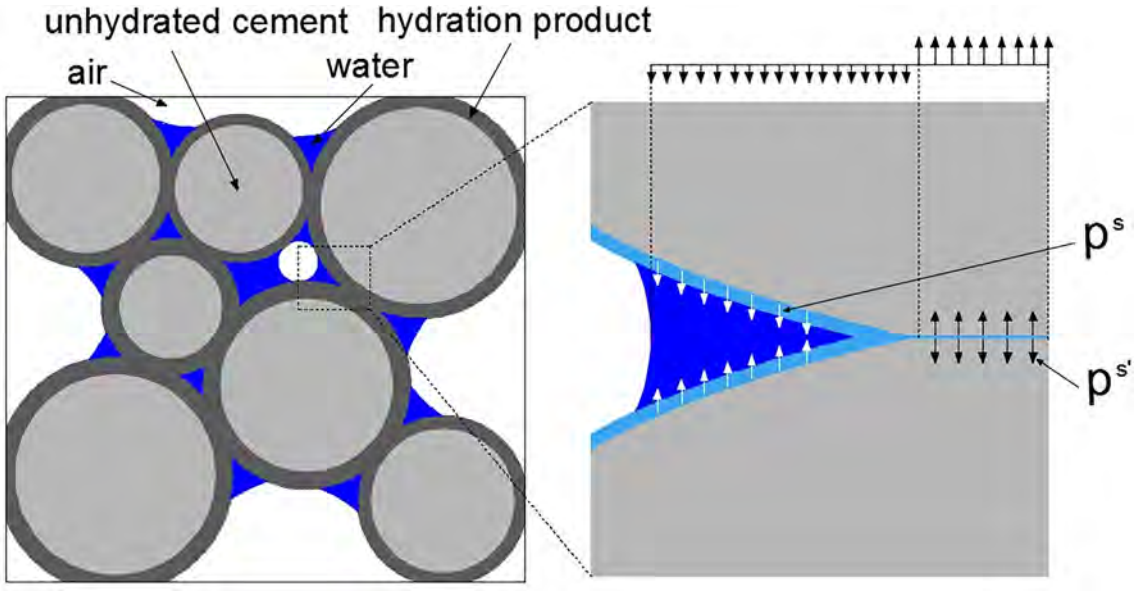

Fig. 3. Schematic representation of the internal pressure $p^s$and resulted compressive pressure $p^{s'}$ in the adsorbed water.

In Equation (18), the elastic and time-dependent part of the autogenous shrinkage of the cement paste are calculated according to the Equations (2) and (10). S_w is calculated with Equation (16) and σ_{cap} with Equation (12). In Fig. 4 a flow chart of the whole calculation procedure is shown.

3. Materials and experiments

In Section 2 a simulation model of autogenous shrinkage has been proposed. In this model, the capillary tension, degree of saturation and elastic modulus are needed to calculate the autogenous shrinkage of cement paste (see section 5). In order to get values for those parameters the internal relative humidity, non-evaporable water content, chemical shrinkage, compressive strength of several cement pastes have to be determined, i.e. measured. The measured setting time and autogenous deformation are used to compare with the calculated autogenous shrinkage by using the proposed model.

Portland cement (CEM I 42.5 N) and Blast furnace slag cement (CEM III/B 42.5N) are used. The Portland cement has a calculated Bogue composition of C_3S 67.1%, C_2S 5.9%, C_3A 7.8%, and C_4AF 9.6%. The mean particle size, D50, of Portland cement and BFS cement are 22 μm and 24 μm. The water-binder ratios are 0.3 and 0.4. The mixture compositions are listed in Table 1. Cement paste is mixed in a 5lL epicyclic Hobart mixer. Demineralized water is mixed with the admixtures and added in two steps to ensure homogeneity of the fresh paste. Total mixing time from first water addition is 3 min.

3.1. Final setting time

After final setting a solid skeleton of cement paste forms. The final setting time is taken as the point from where the driving force of autogenous shrinkage starts to be built up. In this study, the final setting time was determined by the Vicat method according to standard NEN-EN 196-3:2005 [46]. An automatically recording Vicat apparatus was used [47].

3.2. Non-evaporable water content

The non-evaporable water content will be used for calculating the degree of hydration and degree of saturation of the hardening cement paste. For determining the non-evaporable water content, about 10 g of fresh cement paste was placed in a plastic vial. The vials were capped to ensure sealed curing conditions. At the required age, samples for the determination of non-evaporable water content, W_n [g water / g cementitious material], were ground to powder and flushed with liquid nitrogen to stop hydration. The powder was left overnight in an oven at 105 °C (for about 20 h). When removed from the oven, the powder was placed in a furnace at 950 °C for at least 4 h. The non-evaporable water content was calculated as the change of the mass between 105 °C and 950 °C.

3.3. Chemical shrinkage

About 50 g of freshly mixed cement paste was put in an Erlenmeyer flask, with a capacity of 250 ml. After the cement paste was covered with a thin layer of distilled water, the Erlenmeyer flask was filled with paraffin oil and sealed with a rubber stopper encasing a graduated tube with a total volume of 5 ± 0.1 ml. Measurements were performed for 7 days. For each measurement two specimens were tested.

3.4. Internal relative humidity

The development of the internal relative humidity cement of pastes was measured by Rotronic HygroLab C1 equipment with

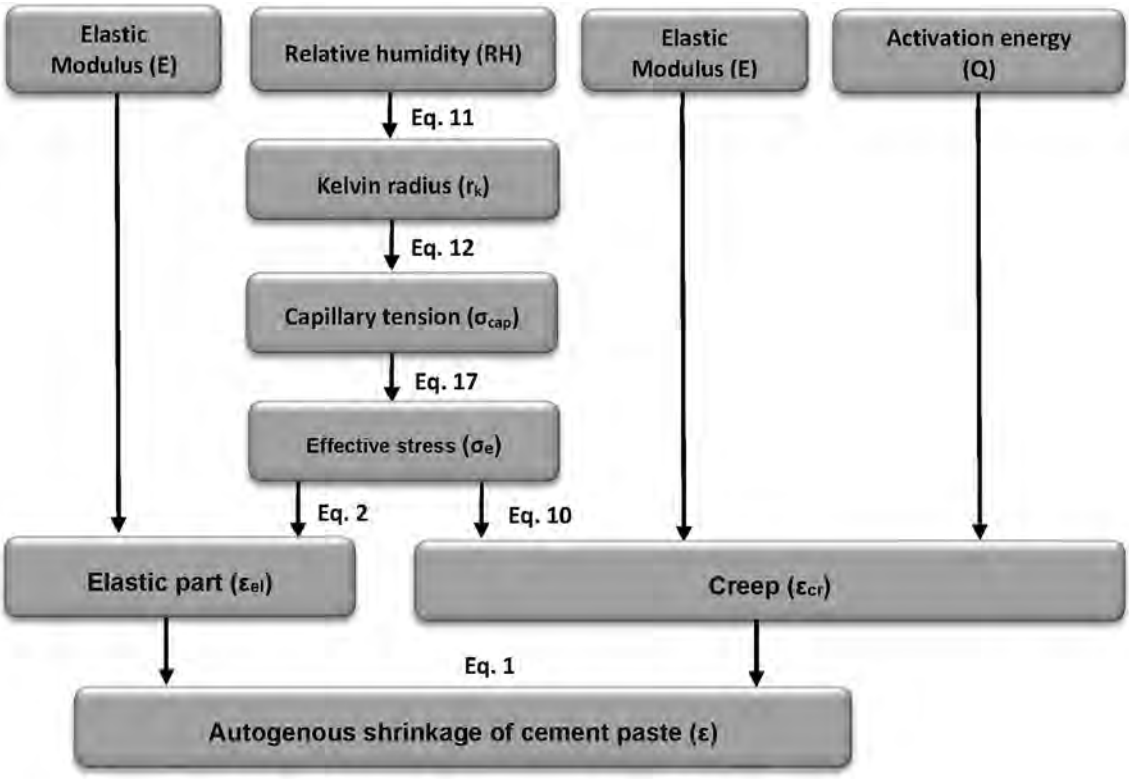

Fig. 4. Scheme of simulation model of autogenous shrinkage.

Table 1
Mixture composition of OPC cement pastes and BFS cement pastes.

Name	CEM I 42.5N (g)	CEM III/B 42.5N (g)	Water (g)	Water/Binder ratio (w/b)
OPC 0.3	1000	0	300	0.3
OPC 0.4	1000	0	400	0.4
BFS 0.3	0	1000	300	0.3
BFS 0.4	0	1000	400	0.4

two HC2-AW RH station probes with an accuracy ±0.5%. The RH in the samples and the temperature were recorded every 2 min. The duration of the test was 7 days.

3.5. Compressive strength

Compressive strength tests were carried out after 1, 3 and 7 days on sealed cured cement paste cubes, 40 × 40 × 40 mm^3. The cubes were cured at 20 °C. At least three specimens were tested for each measurement.

3.6. Autogenous deformation

The cement paste was cast under vibration into tight plastic molds (low-density polyethylene plastic, LDPE), which were corrugated to minimize restraint on the paste [48]. The length of the samples was approximately 430 mm and the diameter 29 mm. Measurements of autogenous shrinkage started after final setting time when a solid skeleton of cement paste was formed. Before that time the specimens were placed on a rotation machine and rotated at a speed of 10 rpm to avoid bleeding. The specimens were placed in a dilatometer and immersed into a temperature controlled glycol bath at 20 ± 0.1 °C. The dilatometer frame consisted of two steel plates joined rigidly by six solid invar rods (diameter 20 mm). Each specimen was longitudinally supported by two parallel rods attached to the steel plates. The specimens were gripped by screws at one end, while the rest could slide freely on the rods, which were lubricated by the glycol bath. The longitudinal deformation was measured at the free end by a TRANS-TEK 350-000 displacement transducer. Three samples were tested in the dilatometer simultaneously, with a measurement accuracy of ±5 μstrain. Length changes were recorded every 5 min.

4. Experimental results and discussion

4.1. Final setting time

In Fig. 5 the final setting times of cement pastes with water-binder ratio of 0.3 and 0.4, cured at 20 °C, are shown. The figure shows that the final setting time is longer for pastes with higher water-binder ratio for both PC and BFS paste. Fig. 5 also shows that the final setting time of CEM III/B 42.5N is shorter than that of CEM I 42.5N. Shorter setting time of BFS cement paste has also been observed by Xiao et al. [49]. This, however, is contradictory to the common understanding that the setting time will increase with increasing slag content. If the Portland cement and BFS cement are made with the same kind of clinker, the lower clinker content in BFS cement results in longer final setting time. According to the producer, CEM I 42.5N and CEM III/B 42.5N used in this study are made with different kind of clinker. CEM III/B 42.5N made with higher activity clinker may have shorter final setting time than that of CEM I 42.5N made with lower activity clinker.

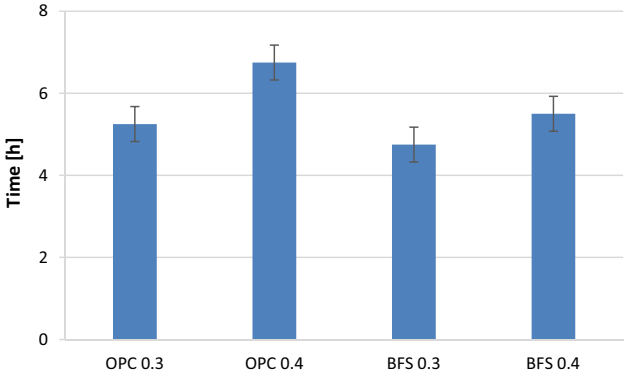

Fig. 5. Final setting time of cement pastes with water-binder ratio of 0.3 and 0.4.

4.2. Non-evaporable water content

The non-evaporable water contents (per gram of original powder) of different kinds of cement paste with water-binder ratio of 0.3 and 0.4 are displayed in Fig. 6 as a function of time. Fig. 6 shows that at the same age the non-evaporable water contents with water binder ratio of 0.4 is higher than that of the same cement pastes with water binder ratio of 0.3. This is due to the higher degree of hydration of cement pastes with water binder ratio of 0.4.

The non-evaporable water content of the BFS cement paste is much lower than that of Portland cement paste with the same water-binder ratio and the same time. The lower non-evaporable water content of the BFS cement paste has two reasons. First, the water binding capacity of BFS is lower than that of Portland cement. According to Gruyaert [50], the water bound by Portland cement at complete hydration is about 0.221 g H_2O /g cement. The non-evaporable water content of BFS cement with 15% Portland cement and 85% BFS at complete hydration is about 0.114 g H_2O /g cement. Second, the hydration rate of BFS during the first seven days is much slower that of Portland cement [51]. A lower degree of hydration of BFS results in a lower non-evaporable water content.

4.3. Chemical shrinkage

Chemical shrinkage will be used for calculating the degree of saturation of cement paste.

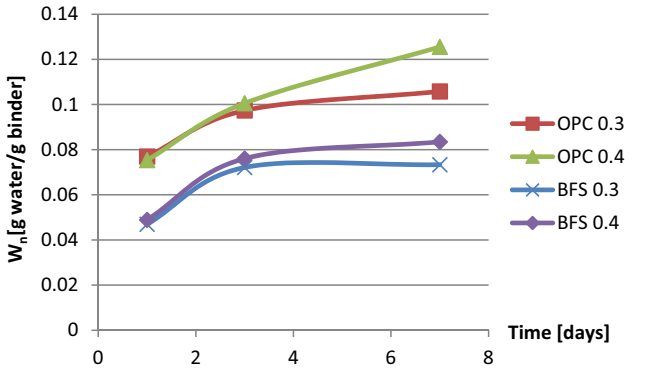

Fig. 6. Non-evaporable water content as a function of age for different cement pastes with water-binder ratio of 0.3 and 0.4.

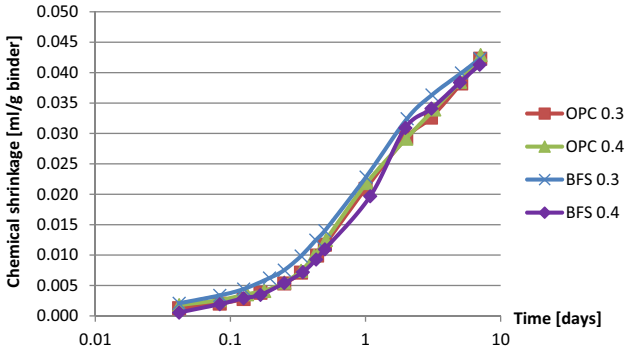

Fig. 7. Chemical shrinkage as a function of age.

Measured chemical shrinkage of Portland and BFS cement pastes is displayed in Fig. 7. Chemical shrinkage of the BFS cement pastes is larger than that of Portland cement pastes in the first 3 days. These results are in line with findings of Bentz [52]. According to Thomas et al. [52] the absolute volume reduction of BFS cement hydration production is larger than that of Portland cement with the same degree of hydration.

4.4. Internal relative humidity

The evolution of the internal relative humidity of the cement pastes with hydration time is provided in Fig. 8. For each series two specimens were tested. The difference between measured internal relative humidity of two specimens was less than 1%. Fig. 8 shows that the moment at which the relative humidity of BFS cement paste starts to drop significantly is later than that of Portland cement paste with the same water-binder ratio. For BFS cement paste with water-binder ratio 0.3 the relative humidity starts to drop 0.6 day later than in the Portland cement paste with water-binder ratio 0.3. For BFS cement paste with water-binder ratio 0.4 the relative humidity starts to drop even 1.5 days later than that of Portland cement paste with water-binder ratio 0.4. A similar result can be found in Lura's thesis [8]. In his thesis the relative humidity of BFS cement paste with water-binder ratio 0.37 starts to drop 1 day later than in the Portland cement paste. The later starting moment of the relative humidity drop of BFS cement paste can be attributed to the low activity of BFS after final setting. BFS cement (CEM III/B 42.5 N) used in the test series contains BFS (66% by mass) and Portland clinker (34% by mass). The large amount of low active BFS in CEM III/B 42.5 N results in lower water consumption of BFS cement during the first few days of hydration and a later starting moment of RH drop of BFS cement paste.

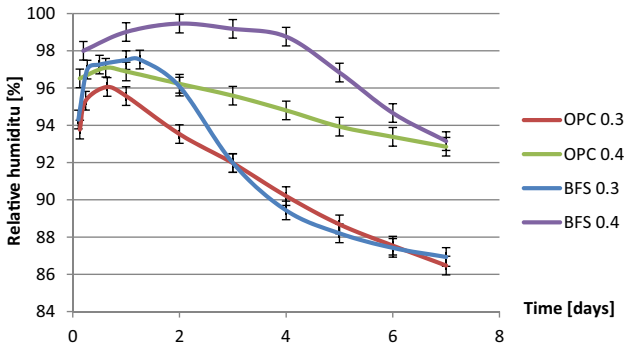

Fig. 8. Internal relative humidity vs. age for different cement paste with water-binder ratio of 0.3 and 0.4.

4.5. Compressive strength

The compressive strength of cement paste will be used to calculate the elastic modulus by using an equation proposed by Takafumi (will be present in Section 5.2). The elastic modulus of cement paste is an important factor in modelling of autogenous shrinkage. Fig. 9 shows the compressive strength as a function of age of cement pastes with water-binder ratio of 0.3 and 0.4.

4.6. Autogenous deformation

Fig. 10 shows the measured autogenous deformations as a function of age of different cement pastes with water-binder ratio of 0.3 and 0.4. For all mixtures a fast shrinkage can be noticed at the beginning. This fast shrinkage is followed by a short period of swelling. After the period of swelling the specimens steadily shrink. According to some researchers [53–55] taking the final setting time as the starting point of autogenous shrinkage is questionable. The starting time of autogenous shrinkage is roughly equal to the setting time, but is not necessarily identical with it [56]. A lot of researchers start counting autogenous shrinkage from 'time-zero', which is defined as the duration between the moment that water comes in contact with cement and the time at which the concrete develops sufficient structure to enable tensile stress transfer through the concrete [57,58]. According to Bjøntegaard [59], the time when the maximum (macroscopic) swelling is observed can be taken as the starting time of autogenous shrinkage ('time-zero'). In this paper the steady shrinkage after (macroscopically) observed maximum swelling is considered as autogenous shrinkage of the cement pastes. The autogenous deformations as a function of age of different cement pastes after early-age swelling is shown in Fig. 11.

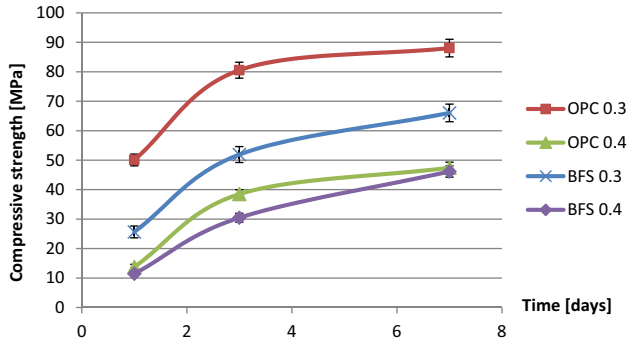

Fig. 9. Compressive strength vs. age for different cement pastes with water-binder ratio of 0.3 and 0.4.

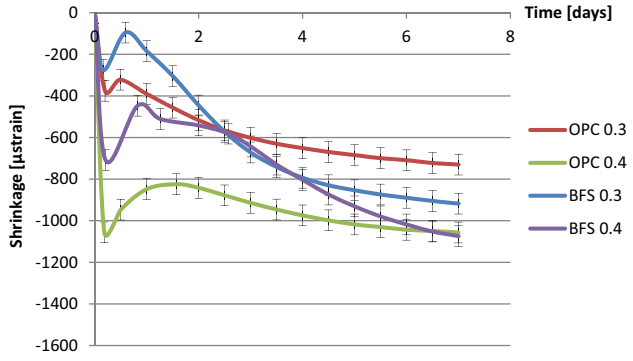

Fig. 10. Autogenous deformation vs. age for cement pastes with water-binder ratio of 0.3 and 0.4 (Starting time: final setting time).

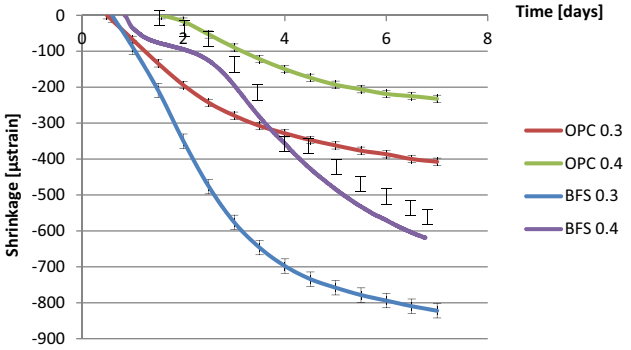

Fig. 11. Autogenous deformation vs. age for cement pastes with water binder ratio of 0.3 and 0.4 (Starting time: after early-age swelling).

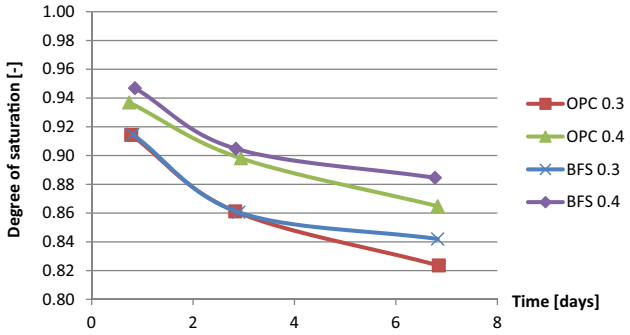

Fig. 12. Calculated degree of saturation as a function of age for cement pastes with water binder ratio of 0.3 and 0.4 (calculated with Equation (16)).

The measured autogenous shrinkage of BFS cement paste is much bigger than that of Portland cement paste with the same water-binder ratio. According to Chan [60], the autogenous deformation of concrete with 40% BFS is significantly higher than that of concrete without BFS. The bigger autogenous shrinkage of BFS cement paste has two reasons. First, the stiffness of BFS cement paste, e.g. elastic modulus, is lower than that of Portland cement paste with same water-binder ratio at the same time. Second, the drop of internal relative humidity of BFS cement paste is larger than that of ordinary Portland cement paste with the same water-binder ratio, as shown earlier in Fig. 8. Similar results are also found by Lura [8] and Ekaputri [61]. According to Ishida et al [62] and Zhang [63], BFS cement pastes have a finer pore structure than Portland cement pastes. Finer pores of BFS cement paste result in a smaller radius of air–water meniscus and larger internal driving force of autogenous shrinkage, e.g. capillary tension.

5. Determination of material parameters used for numerical simulation of autogenous shrinkage

As mentioned in section 3, calculating the autogenous shrinkage of cement paste with the numerical model proposed in Section 2 needs determination of several materials parameters. The materials parameters include degree of saturation, capillary tension and elastic modulus.

5.1. Calculation of the evolution of the degree of saturation

The degree of saturation can be calculated with the measured non-evaporable water content $V_{new}(t)$ and the chemical shrinkage $V_{cs}(t)$ by using Equation (16). The measured non-evaporable water content $V_{new}(t)$ of cement pastes with water-binder ratio 0.3 and 0.4 were shown in Fig. 6 as a function of age. The chemical shrinkage $V_{cs}(t)$ of cement pastes was shown in Fig. 7. The calculated degree of saturation of these four cement pastes with water-binder ratio of 0.3 and 0.4 are shown in Fig. 12 as a function of age.

5.2. Capillary tension

The capillary tension can be calculated from the measured internal relative humidity by using Equations (11) and (12). The starting point of the calculation is the time when the measured internal relative humidity reaches its peak (see Fig. 8) and starts to decrease. Fig. 8 shows that the measured maximum values of the internal relative humidity of different are lower than 100%. This is due to the dissolved ions in the pore fluid [8] and the effect of ions on the relative humidity is assumed as constant in this paper. The calculated capillary tension of cement pastes with water-binder ratio 0.3 and 0.4 is shown as a function of age in Fig. 13.

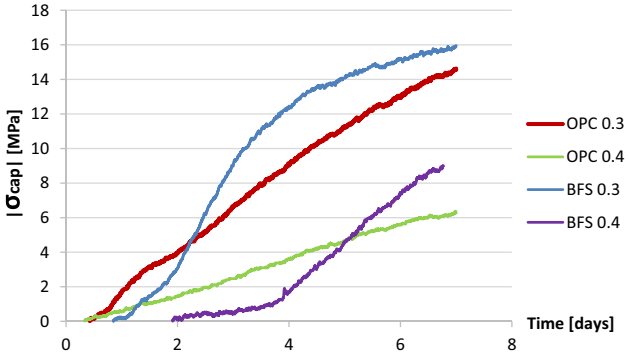

Fig. 13. Calculated capillary tension in the pore water for cement pastes with water-binder ratio of 0.3 and 0.4 as a function of age (calculated with Equation (11) and Equation (12)).

5.3. Elastic modulus

For calculating the elastic part of the autogenous deformation of cement paste the evolution of the elastic modulus is needed. Several equations for predicting the elastic modulus E of cementitious materials as a function of compressive strength $f_c(t)$ have been proposed [64,65]. Among these equations, the equation proposed by Takafumi et al. [65] takes the effect of type of supplementary material on the elastic modulus into consideration. In this paper, this equation is adopted to calculate the elastic modulus E [MPa]. It holds:

$$E(t) = k_1 k_2 \varphi f_c(t)^{1/3} \rho^2 \tag{19}$$

where k_1 [–] is the correction factor related to the type of aggregate. For cement paste,k_1 is taken as 1 because there is no effect of aggregate on the elastic modulus of cement paste. k_2 [–] is a correction factor related to the type of supplementary material, its value for blast furnace slag is 0.95. φ [–] is a fitting coefficient, its value is taken as $\approx$ 0.0015 [65]. ρ [N/m^3] the unit weight of the cement paste.

The elastic modulus of different cement pastes at day 1, day 3 and day 7 can be calculated by using Equation (19). Based on these calculated results, logarithmic equations of evolution of elastic modulus of different cement pastes can be obtained. The elastic modules of cement pastes at other hydration times can be calcu-

lated by using these logarithmic equations. The calculated elastic modulus of different cement pastes is shown in Fig. 14.

6. Numerical simulation of autogenous shrinkage

The calculated degree of saturation, capillary tension and elastic modulus are used in the proposed simulation model to predict the autogenous shrinkage of OPC and BFS cement pastes following the schedule shown in Fig. 4. The calculated autogenous shrinkages of different cement pastes are compared with experimental results to evaluate the accuracy of the predictions with the model.

6.1. Portland cement pastes with w/b ratio 0.3 and 0.4

Fig. 15(a) and 16(a) show the measured and calculated autogenous deformation of ordinary Portland cement pastes with water-binder ratio 0.3 and 0.4 after the final setting time. The measured values of autogenous shrinkage are shown from the moment of final setting time. A fast shrinkage can be noticed after final setting. As explained in Section 4.6, taking the moment of final setting as the starting point of autogenous shrinkage is questionable. Therefore, in this section the measured autogenous shrinkage after maximum swelling of the cement paste is used for comparison with the simulation results. In Figs. 15(b) and 16(b), autogenous shrinkages of Portland cement pastes with water-binder ratio 0.3 and 0.4 after the short period of swelling are presented. In the latter figures, the calculated contributions of elastic and time-dependent part of autogenous shrinkage are shown as well. The time step of the calculation is 2 min which is the same as the time interval of the measured internal relative humidity.

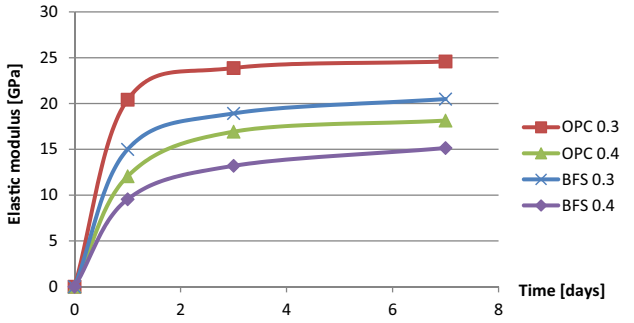

Fig. 14. Calculated elastic modulus vs. age of cement pastes with water-binder ratio of 0.3 and 0.4 (calculated with Equation (19)).

6.2. Blast furnace slag cement pastes with w/b ratio 0.3 and 0.4

Figs. 17 and 18 show the measured and calculated autogenous shrinkage of BFS cement pastes with water-binder ratio 0.3 and 0.4. Fig. 17(a) and 18(a) show the measured and calculated autogenous deformation of BFS cement paste with water-binder ratio 0.3 and 0.4 after the final setting time. The calculated autogenous shrinkage of BFS cement paste after early-age swelling are shown in Fig. 17(b) and 18(b), subdivided in an elastic part and a creep part.

6.3. Discussion

Fig. 15(b), 16(b), 17(b) and 18(b) show the simulated autogenous shrinkage of OPC and BFS cement pastes after maximum swelling. It can be noticed that the simulated autogenous shrinkages of cement pastes at the first several days are generally smaller than the measured results. As discussed in Section 2.2.1, different mechanisms have been proposed as the cause of autogenous shrinkage. However, in this paper only capillary tension is calculated in the proposed model. Without taking other mechanisms into consideration may lead to underestimated internal driving force and autogenous shrinkage.

In this paper the simulated autogenous shrinkage includes an elastic part and a creep part. In order to illustrate the importance of the creep part of autogenous shrinkage, blast furnace slag cement paste with water-binder ratio of 0.3 is taken as an example. As shown in Fig. 19(a) if only the elastic part is considered and the creep part is neglected, the calculated autogenous shrinkage is much smaller than the measured autogenous shrinkage. This result is in line with the finding reported by Lura [8]. In Lura's thesis, the autogenous shrinkage of the BFS cement paste with water-binder ratio of 0.37 was studied. Lura simulated the autogenous shrinkage

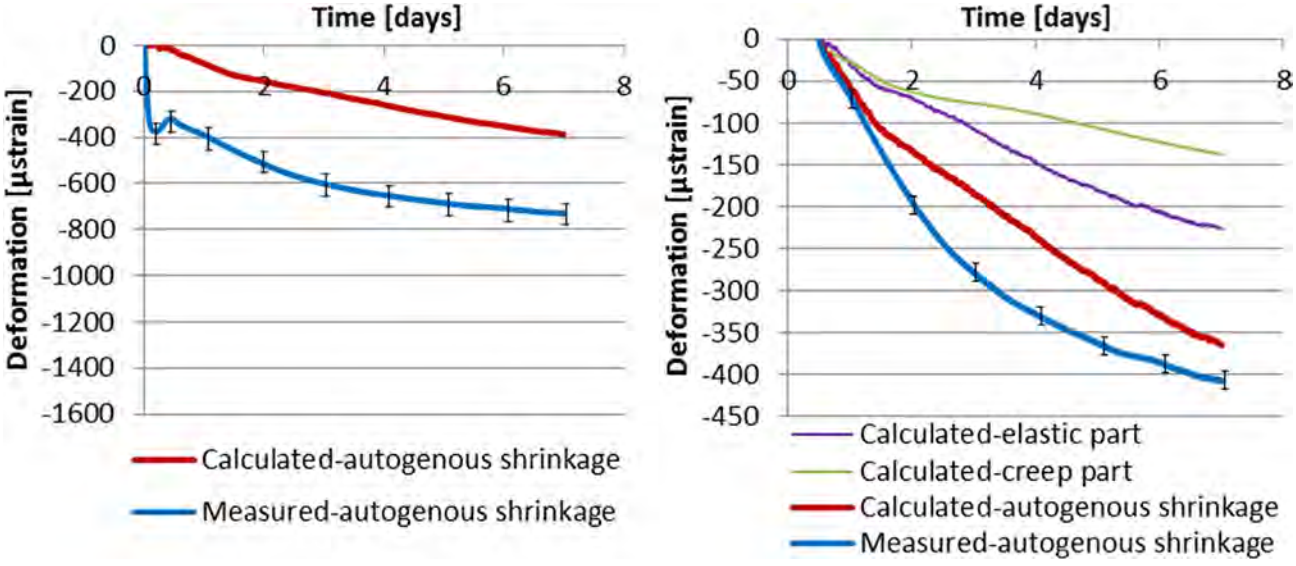

(a) Starting time: final setting time (b) Starting time: after maximum swelling

Fig. 15. Measured and calculated autogenous deformation of Portland cement paste with water-binder ratio 0.3 (Note: Vertical scales are different).

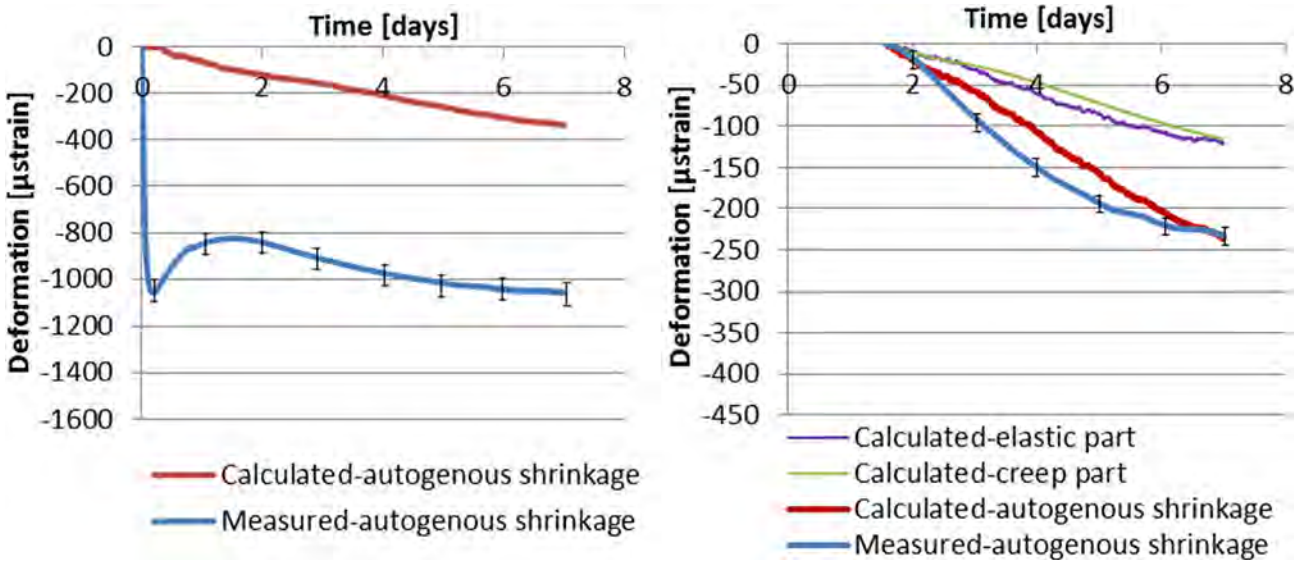

(a) Starting time: final setting time (b) Starting time: after maximum swelling

Fig. 16. Measured and calculated autogenous deformation of Portland cement paste with water-binder ratio 0.4 (Note: Vertical scales are different).

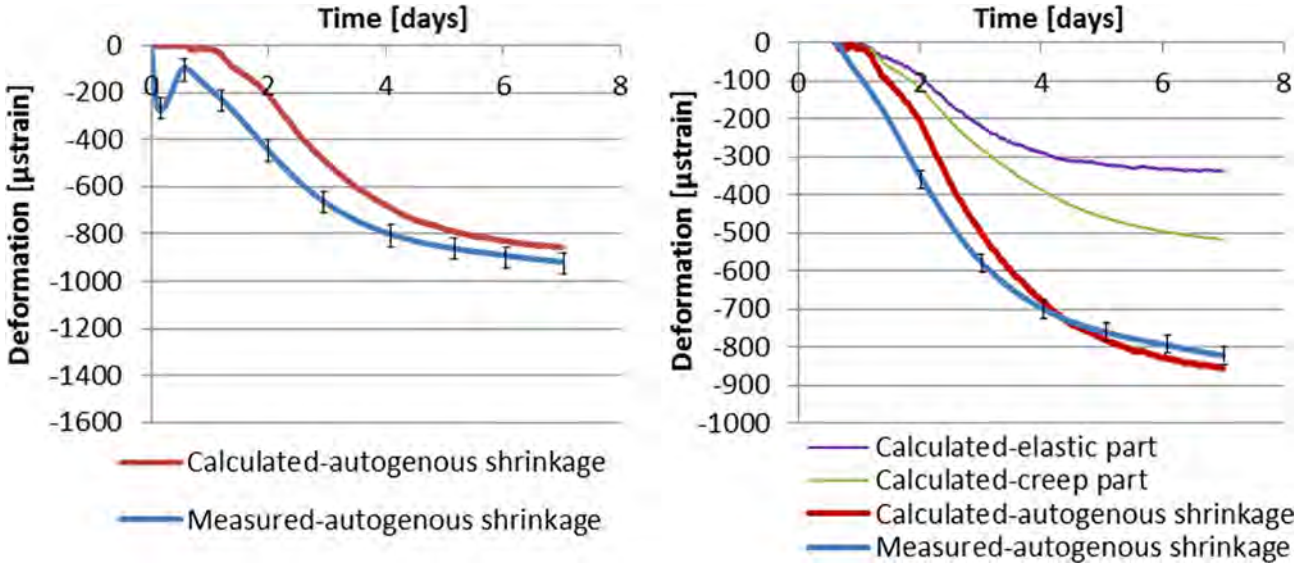

(a) Starting time: final setting time (b) Starting time: after maximum swelling

Fig. 17. Measured and calculated autogenous deformation of blast furnace slag cement paste with water-binder ratio 0.3 (Note: Vertical scales are different).

of BFS cement paste assuming the cement paste to perform as an elastic material. The calculated and measured autogenous shrinkage are shown in Fig. 19(b). By taking the creep into consideration the simulation model predicts the autogenous shrinkage of BFS cement paste with water-binder ratio of 0.3 quite well (Fig. 19 (a)). This finding is in line with Hu [19] who also reported the good prediction of the autogenous shrinkage by taking the creep into account.

7. Concluding remarks

In this paper, a simulation model for autogenous shrinkage of cement paste is proposed. In this model, the autogenous deformation has been split up in an elastic and a time-dependent component. The elastic component is calculated by Hooke's law. The time-dependent component is based on the activation energy concept. The autogenous shrinkage of OPC and BFS cement pastes is predicted by using the proposed model and compared with the measured results. The following remarks can be made:

(1) In this paper, the autogeous shrinkage of OPC and BFS cement pastes are studied. The measured autogenous shrinkage of BFS cement paste is much bigger than that of Portland cement paste with same water-binder ratio. The change of internal relative humidity of BFS cement pastes is much bigger than that of Portland cement pastes with

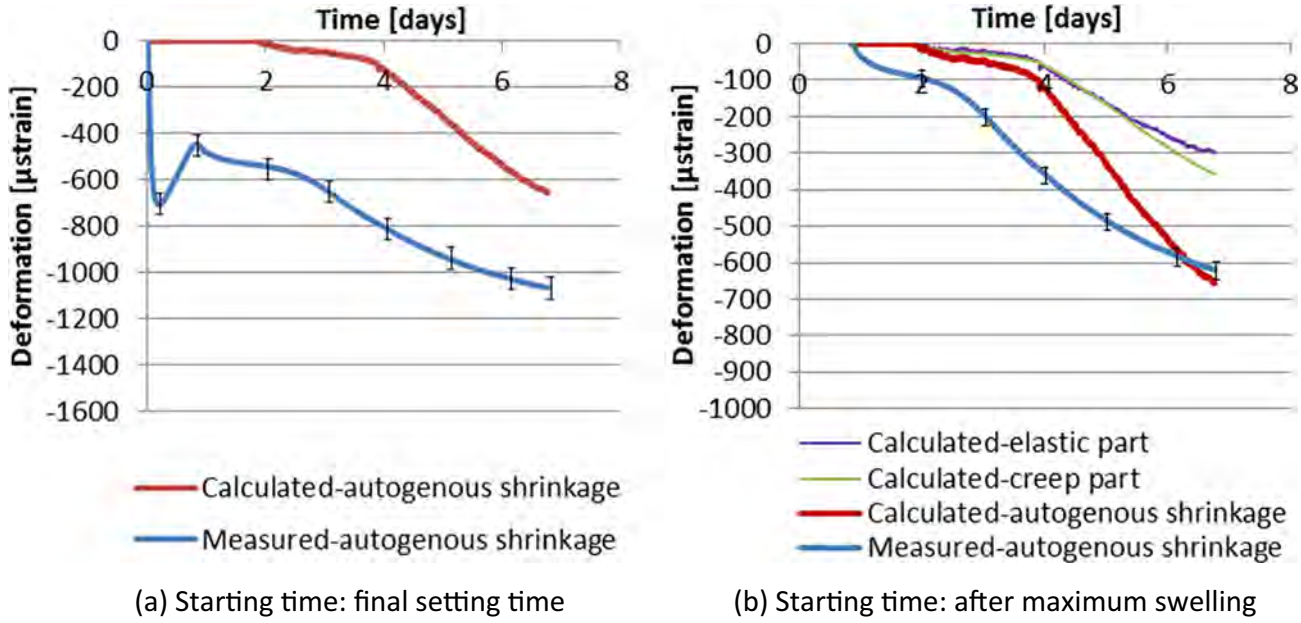

(a) Starting time: final setting time (b) Starting time: after maximum swelling

Fig. 18. Measured and calculated autogenous deformation of blast furnace slag cement paste with water-binder ratio 0.4 (Note: Vertical scales are different).

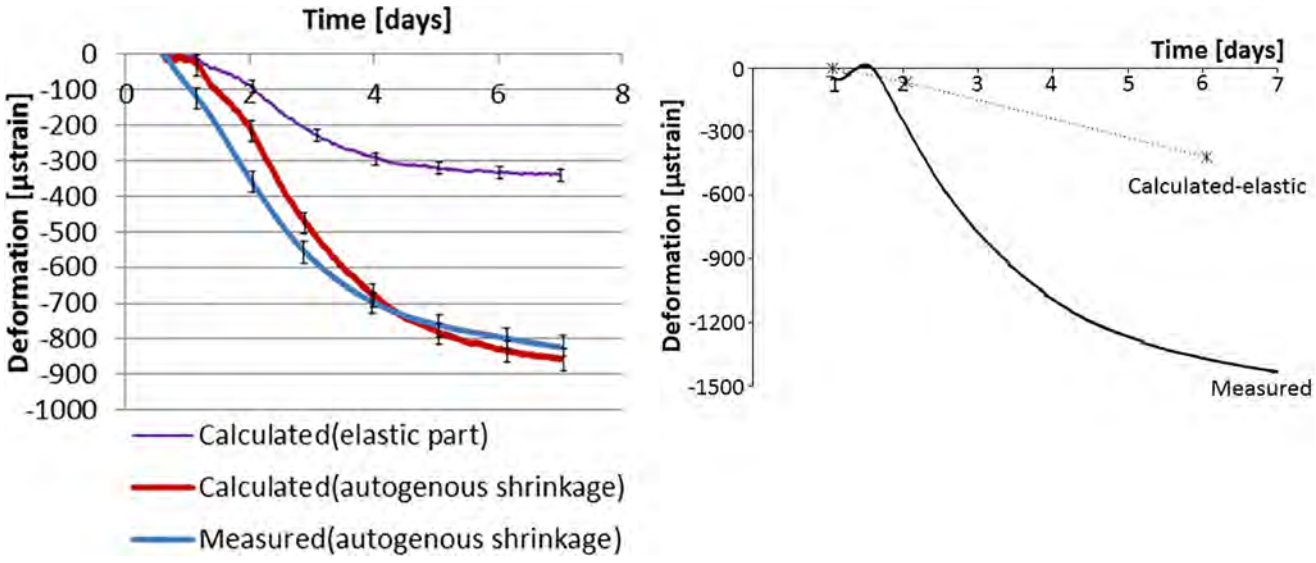

(a) Simulation result of this thesis (b) Simulation result of Lura (2003)

Fig. 19. Measured and calculated autogenous deformation of blast furnace slag cement paste with water binder ratio of 0.3.

same water-binder ratio at the same curing age. A bigger drop of the relative humidity of BFS cement paste results in bigger capillary tension. The bigger capillary tension and smaller resistance to deformation result in bigger autogenous shrinkage of BFS cement paste.

(2) In studies on the autogenous shrinkage cement paste is often considered as a continuously changing elastic material. However, the early-age cement paste is a visco-elastic material. The time-dependent behaviour of the material, i.e. creep, plays a significant role in the early-age autogenous shrinkage as well. The contribution of creep to autogenous shrinkage increases with time. In this research, the effect of creep on autogenous shrinkage of cement paste is studied. The calculated autogenous shrinkage (with creep) of cement paste is compared with measurements. The comparison between the calculated autogenous shrinkage of cement paste and the measured result shows the simulation model predicts the trend of autogenous shrinkage of Portland and Blast furnace slag cement pastes with water binder ratio of 0.3 and 0.4 quite well.

CRediT authorship contribution statement

Tianshi Lu: Conceptualization, Methodology, Investigation, Software, Writing - original draft. **Zhenming Li:** Writing - review

& editing. **Klaas van Breugel:** Supervision, Writing - review & editing.

Declaration of Competing Interest

The authors declare that they have no known competing financial interests or personal relationships that could have appeared to influence the work reported in this paper.

Acknowledgment

Tianshi Lu would like to acknowledge the funding supported by the China Scholarship Council (CSC) and Delft University of Technology (TU Delft).

References

[1] M.S. Sule, Effect of Reinforcement on Early-Age Cracking in High Strength Concrete, Ph.D. Thesis. (2003).
[2] B.F. Dela, Eigenstresses in hardening concrete, Ph.D. thesis. (2000).
[3] A.M. Paillere, M. Buil, J.J. Serrano, Effect of fiber addition on the autogenous shrinkage of silica fume concrete, ACI Mater. J. 86 (1989) 139–144.
[4] E. Tazawa, S. Miyazawa, Influence of cement and admixture on autogenous shrinkage of cement paste, Cem. Concr. Res. 25 (1995) 281–287.
[5] Japan Concrete Institute Committee on Autogenous Shrinkage, Report on Autogenous Shrinkage of Concrete, Proc. Int. Workshop Autoshrink '98, (1999) 1-67.
[6] T.C. Powers, Mechanisms of shrinkage and reversible creep of hardening cement paste, in Proc. Int. Symp. Structure of Concrete and its behaviour under load, Cem. Concr. Ass., (1965) 319-344.
[7] D.P. Bentz, E.J. Garboczi, D.A. Quenard, Modelling drying shrinkage in reconstructed porous materials: application to porous Vycor glass, Modelling and Simulation in Materials Science and Engineering 6 (1998) 211–236.
[8] P. Lura, Autogenous deformation and internal curing of concrete. Ph.D. Thesis. (2003).
[9] Y. Wei, W. Hansen, J.J. Biernacki, E. Schlangen, Unified shrinkage model for concrete from autogenous shrinkage test on paste with and without ground-granulated blast-furnace slag, ACI Mater. J. 108 (2011) 12–20.
[10] C. Hua, P. Acker, A. Erlacher, Analyses and models of the autogenous shrinkage of hardening cement paste: I, Modelling at macroscopic scale, Cem Concr Res 25 (1995) 1457–1468.
[11] B. Person, Creep and shrinkage of young or mature HPC. In Proc. 5th Int. Symp. on 'Utilization of high strength/high performance concrete', (1999) 1272-1281.
[12] D. Gawin, F. Pesavento, B.A. Schrefler, Modelling creep and shrinkage of concrete by means of effective stresses, Mater Struct 40 (2007) 579–659.
[13] Z. Li, T. Lu, X. Liang, H. Dong, G. Ye, Mechanisms of autogenous shrinkage of alkali-activated slag and fly ash pastes, Cem. Concr. Res. 106107 (2020).
[14] T. Lu, Autogenous deformation of early age cement paste and mortar. Ph.D. Thesis. (2019).
[15] A.M. Neville, W.H. Dilger, J.J. Brooks, Creep of Plain and Structural Concrete, Construction Press, 1983.
[16] R.I. Gilbert, Time effects in concrete structures. Series: Developments in civil engineering 23(1988).
[17] S.J. Lokhorst, K. van Breugel, Simulation of the effect of geometrical changes of the microstructure on the deformational behaviour of hardening concrete. Cement and concrete research 27(1997) 1465-1479.
[18] A. Aili, M. Vandamme, J.M. Torrenti, B. Masson, A viscoelastic poromechanical model for shrinkage and creep of concrete, Cem. Concr. Res. 129 (2020) 105970.
[19] Z. Hu, Prediction of autogenous shrinkage in fly ash blended cement systems, PhD thesis (2017).
[20] S. Timoshenko, J. N. Goodier, Theory of elasticity, 2nd Edition. McGraw-Hill Book Co., Inc., New York(1951).
[21] L.F. Nielsen, A research note on sorption, pore size distribution, and shrinkage of porous materials, TR 245/91, Building Materials Laboratory, The Technical University of Denmark, Lyngby, Denmark (1991).
[22] W. Soboyejo, Mechanical Properties of Engineered Materials (2002).
[23] G.A. Hirst, A.M. Neville, Activation energy of creep of concrete under short-term static and cyclic stresses, Magazine Concr. Res. 29 (1977) 13–18.
[24] Z.P. Bazant, F.H. Wittmann, Creep and shrinkage in concrete structures, (1982) 12-16.
[25] R.L. Day, B.R. Gamble, The effect of changes in structure on the activation energy for the creep of concrete, Cem. Concr. Res. 13 (1983) 529–540.
[26] P. Klug, F. Wittmann, Activation energy of creep of hardened cement paste, Matér. Constr. 2 (1969) 11–16.
[27] F.H. Wittmann, Surface tension, shrinkage and strength of hardened cement paste, Mater. Struct. 1 (1968) 547–552.
[28] P. Klug, F. Wittmann, Activation energy and activation volume of creep of hardened cement paste, Mater. Sci. Eng. 15 (1974) 63–66.
[29] F.H. Wittmann, Kriechverformung des Betons unter statischer und unter dynamischer Belastung, Rheol. Acta 10 (1971) 422–428.
[30] F.H. Wittmann, Kriechmessungen an Zementstein, Rheol. Acta 6 (1967) 303–306.
[31] F.H. Wittmann, On the interaction of gel particles in hydrating Portland cement, Hydration and Setting of Cements, ed. A. Nonat & J.C. Mutin, RILEM, E&FN Spon, London(1992).
[32] M.J. Setzer, The Munich model – an example for modern materials science in civil engineering, Adv. Build. Mater. Sci. (1996) 3–16.
[33] O.M. Jensen, Thermodynamic limitation of self-desiccation, Cem. Concr. Res. 25 (1995) 157–164.
[34] F.H. Wittmann, Heresies on shrinkage and creep mechanisms. Proceedings of Creep, Shrinkage and Durability Mechanics of Concrete and Concrete Structures, London: Taylor and Francis Group, (2009) 3-10.
[35] Y. Wei, Modeling of autogenous deformation in cementitious materials, restraining effect from aggregate, and moisture warping in slabs on grade. Ph.D. Thesis. (2008)
[36] C. Di Bella, M. Wyrzykowski, P. Lura, Evaluation of the ultimate drying shrinkage of cement-based mortars with poroelastic models. Mater. Struct., 50 ((2017), 52.
[37] H.J. Butt, M. Kappl, Normal capillary forces, Adv. Colloid Interface Sci. 146 (2009) 48–60.
[38] O.M. Jensen, Autogenous deformation and RH-change – self-desiccation and self-desiccation shrinkage (in Danish), TR 284/93, Building Materials Laboratory, The Technical University of Denmark, Lyngby, Denmark (1993).
[39] R. Defay, I. Prigogine, Surface Tension and Adsorption. Longmans, Green & Co Ltd, London (1966).
[40] A.W. Skempton, Effective stress in soils, concrete and rocks, Pore Pressure and Suction in Soils, Butherworths,London, (1961) 4–16.
[41] W.G. Gray, B.A. Schrefler, Thermodynamic approach to effective stress in partially saturated porous media, Eur. J. Mech. A/Solids 20 (2001) 521–538.
[42] M.M. Alam, M.K. Borre, I.L. Fabricius, K. Hedegaard, B. Røgen, Z. Hossain, A.S. Krogsbøll, Biot's coefficient as an indicator of strength and porosity reduction: Calcareous sediments from Kerguelen Plateau, J. Petroleum Sci. Eng. 70 (2010) 282–297.
[43] T.C. Powers, T. L. Brownyard, Studies of the physical properties of hardened Portland cement paste (9 parts), J Amer Concr Inst 43 (Oct. 1946 to April 1947), Bulletin 22, Research Laboratories of the Portland Cement Association, Chicago (1948).
[44] K. van Breugel, Simulation of hydration and formation of structure in hardening cement-based materials, Ph.D. thesis (1991).
[45] Q. Zeng, K. Li, T. Fen-Chong, P. Dangla, Pore structure characterization of cement pastes blended with high-volume fly-ash, Cem. Concr. Res. 42 (2012) 194–204.
[46] NEN-EN 196-3, Methods of Testing Cement. Part 3: Determination of Setting Times and Soundness (2005).
[47] T. Lu, Z. Li, H. Huang, Effect of supplementary materials on the autogenous shrinkage of cement paste, Materials 13 (15) (2020) 3367.
[48] Standard, A. S. T. M. Standard test method for autogenous strain of cement paste and mortar. ASTM C-1698 (2009).
[49] K.T. Xiao, H.Q. Yang, Y. Dong, Study on the influence of admixture on chemical shrinkage of cement based materials. In Key Engineering Materials. Trans Tech Publications. Vol. 405(2009) 226-233.
[50] E. Gruyaert, Effect of blast-furnace slag as cement replacement on hydration, microstructure, strength and durability of concrete. Ph.D. thesis (2011).
[51] H. Taylor, Cement Chemistry, Academic Press, London, 1992.
[52] J.J. Thomas, A.J. Allen, H.M. Jennings, Density and water content of nanoscale solid C-S–H formed in alkali-activated slag (AAS) paste and implications for chemical shrinkage, Cem. Concr. Res. 42 (2012) 377–383.
[53] C.W. Miao, Q. Tian, W. Sun, J.P. Liu, Water consumption of the early-age paste and the determination of "time-zero" of self-desiccation shrinkage, Cem. Concr. Res. 37 (2007) 1496–1501.
[54] A. Bentur, Terminology and definitions, in: K. Kovler, A. Bentur (Eds.). International RILEM Conference on Early Age Cracking in Cementitious Systems—EAC, RILEM TC181-EAS, Haifa (2002) 13–20.
[55] G. Sant, F. Rajabipour, P. Lura, J. Weiss, Examining time-zero and early age expansion in pastes containing shrinkage reducing admixtures (SRA's). In Proc., 2nd RILEM Symp. on Advances in Concrete through Science and Engineering (2006).
[56] A. Bentur, Terminology and Definitions, RILEM Report 25, Early Age Cracking in Cementitious Systems, Edited by A. Bentur, RILEM Publications S.A.R.L., Cachan, France, (2003) 13-15.
[57] J. Weiss, Experimental Determination of the 'Time Zero' to (Maturity-Zero Mo), RILEM Report 25, Early Age Cracking in Cementitious Systems, Edited by A. Bentur, RILEM Publications S.A.R.L., Cachan, France, (2003) 195-206.
[58] K. Kovler, D. Cusson, Effects of internal curing on autogenous deformation. Internal Curing of Concrete-State-of-the-Art Report of RILEM Technical Committee 196-ICC, (2007) 71-104.
[59] Ø. Bjøntegaard, Thermal dilatation and autogenous deformation as driving forces to self-induced stresses in high performance concrete, Ph.D. Thesis (1999).

[60] Y.W. Chan, C.Y. Liu, Y.S. Lu, Effects of slag and fly ash on the autogenous shrinkage of high-performance concrete, in Proceedings of International Workshop Autoshrink'98, London(1999) 221-228.
[61] J.J. Ekaputri, K. Maekawa, T. Ishida, Experimental study on internal RH of BFS mortars at early age, Mater. Sci. Forum 857 (2016).
[62] T. Ishida, Y. Luan, T. Sagawa, Modeling of early age behavior of blast furnace slag concrete based on micro-physical properties, Cem. Concr. Res. 41 (12) (2011) 1357–1367.
[63] Y. Zhang, Non-saturated chloride diffusion in sustainable cementitious materials, Ph.D. Thesis (2018).
[64] ACI Committee 363, State-of-the-Art Report on High-StrengthConcrete, ACI JOURNAL, Proceedings V. 81, No. 4, July-Aug.1984 (1984) 364-411.
[65] N. Takafumi, T. Fuminori, M.K. Nemati, M.C. Bernardino, P.F. Alessandro, A Practical Equation for Elastic Modulus of Concrete, ACI Struct. J., V. 106, No. 5, Sept.-Oct. (2009) 690-696.